Acta Translational Medicine *An International Scientific Journal*	ISSN: 2521-8662	Volume 5	Issue 1	Pp19-28	January 2022

APPLICATION OF ARTIFICIAL INTELLIGENCE MULTIMODAL ULTRASONOGRAPHY FOR PREDICTING THE RISK OF ACUTE KIDNEY INJURY IN SEPSIS

Piotr Materzok

University of Wrocław,Poland

Email: 2021004022@poers.edu.pl

Abstract

The occurrence of acute kidney injury in sepsis represents a common complication in hospitalized and critically injured patients that is usually associated with negative prognosis, which presents additional consequences in terms of the risk of developing chronic kidney disease coupled with significantly higher mortality. To intervene prematurely in high-risk patients, improve poor prognosis and further enhance the success rate of resuscitation in severe cases, a diagnostic grading standard of acute kidney injury is employed as the basis in this paper. Firstly, an artificial intelligence multimodal ultrasound imaging technique is conceived by incorporating conventional ultrasound, ultrasonography and shear wave elastography examination approaches. Secondly, the acquired focal lesion images in the kidney lumen are mapped into a knowledge map and then injected into feature mining of a multicenter clinical dataset to accomplish risk prediction for the occurrence of acute kidney injury. Eventually, the clinical decision curve demonstrated that the application of the prediction model can provide net benefits to patients in the range of 0.017 to 0.89 for threshold probability fluctuations. Additionally, the values of model sensitivity, specificity, accuracy, and AUC are 67.9%, 82.48%, 76.86%, and 0.692, respectively, which confirms out that multimodal ultrasonography not only improves the diagnostic sensitivity of the model, but also dramatically raises the risk prediction ability, illustrating that the predictive model possesses promising validity and accuracy.

Keywords: Artificial intelligence; multimodal ultrasonography; sepsis; acute kidney injury; risk forecast

1 INTRODUCTION

The acute kidney injury is a common disease presenting with complex etiology, diverse clinical manifestations, high morbidity and mortality rates, high treatment costs, and can lead to serious disease development such as death (Kunitsu et al.,2022) The incidence of acute kidney injury in ICU is as high as 6.1%-70.2%, and in-hospital complication rates and morbidity and mortality are significantly increased (Gong ., et al.,2022) as well as can lead to longer hospital stays, additional costs, and poor prognosis. Besides, most patients developed acute kidney injury within two days of study enrollment(Alejandra et al.,2022) Patients with acute kidney injury have a high mortality rate that is often underestimated in clinical practice with increasing length of hospital stay (Shao et al.,2022) . To a certain extent, the diagnostic criteria of acute kidney injury have deepened the understanding of the probability and course of acute kidney injury in patients (Xue et al.,2021) However, the effects of treatment and intervention in early identification of the condition vary widely.

Currently, the occurrence of acute kidney injury is mainly determined based on changes in functional indicators of serum creatinine (Hu et al.,2022). According to studies, serum creatinine is not well sensitive to acute changes in renal function, and levels can vary widely with muscle mass, diet, age, hydration status, medications, and gender (Zhang et al.,2020). In addition, it does not act as a marker of renal tubular damage. A marked increase in serum creatinine can be found when renal blood pressure is too low, leading to prerenal azotemia, even if there is no loss of renal tissue. For these reasons, serum creatinine is often defined as the criterion for deficient acute kidney injury(Ig et al.,2021) . Another problem with serum creatinine is that true baseline values are generally not available in most clinical stages. Given the phenotypic variability of acute kidney injury, there is uncertainty about the necessity of different methods to diagnose and monitor the clinical course and treatment (Lazzareschi et al.,2023). Meanwhile, urine output is influenced by glomerular filtration rate, diuretics and other factors. As indicators for judging the occurrence of nephropathy, there are still many shortcomings in both of them, lacking sensitivity and specificity, failing to reflect early and accurate changes in renal function yet, and consequently delaying diagnosis and treatment.

Several biomarkers of kidney injury contribute significantly to early detection of acute kidney injury (Zeng et al.,2020). Such novel markers include KIM-1 etc, which are yet to be routinely available for clinical practice (Wu., et al.,2022;Zeng et al.,2019;Zeng et al.,2014;Zeng et al.,2013). Biomarker-based strategies are relatively expensive and have not been appropriately applied owing to the clinical heterogeneity displayed by individual patients (González et al.,2022). There is still no effective treatment for acute kidney injury, hence early identification and active prevention are particularly essential. Therefore, it is necessary to investigate a predictive method of predicting potential trends in such disorders to identify high-risk individuals for early prevention.

Acute kidney injury prediction is a research hotspot in recent years. Literature (El-Sadek et al.,2020) divided several severely ill neonates into three groups. Group 1 has significantly higher mean cystatin C levels on day 1of incubation. Moreover, serum creatinine and RRI are not dramatically different between all groups. At a certain critical value, the area under the curve of cystatin C level (0.804) was significantly higher than that of serum creatinine and RRI, which has 53.3% sensitivity and 100% specificity in early prediction of AKI neonates. RRI possesses the low non-significant AUC at the threshold of 0.53 (0.551) , which has 100% sensitivity and 40% specificity, while at the other threshold with 33.3% sensitivity and 86.7% specificity. Ref. (Zdziechowska et al.,2021) reviewed the pathophysiology and suggested the best markers that can effectively predict contrast-induced acute kidney injury. Ref. (Raman et al.,2020) explored the variables that may predict the development of acute kidney injury on the day of admission for children from birth to less than 16 years of age admitted to hospital between 2015 and 2018. Measurements and primary outcomes showed that, adjusted odds ratio for disease occurrence is 4.2 and adjusted odds ratio in the non-cardiac cohort is 7.3. Ref. (Titus et al.,2022) employed data from spatial cohorts to determine hematological markers. Cox regression is conducted after dividing the rates into tertiles. One-month mortality, described by the Kaplan-Meier curve, was used as a significant predictor in Cox analysis. Studies have found that hematological ratios can be used as risk predictors of AKI. Ref.(Trongtrakul et al.,2020) developed AKI prediction scores utilizing data from critically injured patients undergoing non-cardiothoracic surgery in Thai surgical ICU study. As results showed, the model included 3474 surgically critically injured patients and 333 (9.6%) developed AKI. This approach functions favorably to predict AKI in critically injured patients undergoing non-cardiothoracic surgery. It is evident that the existing prediction method has high feasibility and utility to allow better prediction for the probability of AKI in patients and plays a significant role in preventing AKI.

Sepsis is the most common cause of death in intensive care unit, and sepsis with AKI has a higher risk of death. Therefore, in this paper, the diagnostic criteria for AKI is divided into three grades. Firstly, a multimodal ultrasonography technique consisting of conventional ultrasound, ultrasonography, and shear wave elastography examination method is applied to acquire focal lesion images in kidney cavity and construct a knowledge map. Secondly, a model for risk prediction is designed employing knowledge feature extraction, patient feature representation, and a multicenter discriminator. Thirdly, the development of a tool for risk prediction aims to support clinicians intervene with patients as well as reduce the incidence of such, thereby further reducing the progression to ESRD and mortality in surviving patients.

2 DIAGNOSTIC CRITERIA FOR THE OCCURRENCE OF AKI IN SEPSIS

AKI is caused by lots of factors, and kidney function can decline within hours. As a consequence, it is often characterized by a rapid decrease in glomerular filtration or accumulation of nitrogenous waste products in the body, which contributes to blood loss or shock in patients with severe sepsis and disorders of water, electrolyte, and acid-base balance in body (Liu et al.,2020) . Acute kidney injury has a short onset and severe deterioration, often manifesting as clinical complications or syndromes. According to global kidney disease prognosis improvement organization, acute kidney injury is defined as abnormalities in blood, urine, histology and imaging (Ostermann et al.,2020). The duration of the disease is usually less than three months and the basis for diagnosis is illustrated in Table 1. In this case, the SCR first collected on admission is taken as the baseline value when historical SCR baseline values are not available for patients. It can be concluded that the grading criteria for acute kidney injury can be defined as grade three. Patients are also included in tertiary staging if they are treated with RRT or younger than 18 years old with GFR less than 31 ml/min/m^2.

Table 1 Diagnostic criteria for AKI

Standard classification		Index	Details
Comprehensive standard		SCR	Increase by more than 27.5μmol/L within 48 hours, and 1.8 times or more than baseline within one week
		Urine output	Less than 0.46ml/kg*h, the duration is not less than 5 hours
Staging standard	Phase 1	SCR	1.6 times the basal value or increased to 27.1μmol/L
		Urine output	Less than 0.46ml/kg*h, the duration is 5~10 hours
	Phase 2	SCR	2.3 times the base value
		Urine output	Per hour less than 0.46ml/kg for more than 10 hours
	Phase 3	SCR	More than 2.3 times the basal value or increased to 427.1μmol/L
		Urine output	Per hour less than 0.26ml/kg for more than 1 day or anuria for more than 12 hours

Acute kidney injury is treated with fluid therapy, administering vasoactive drugs, controlling infection and avoiding nephrotoxic drugs. As the indicators measured during the patient's hospitalization are repetitive and varied, there is some variability from patient to patient.

3 RISK PREDICTION MODEL BASED ON MULTIMODAL ULTRASONOGRAPHY

3.1 Intracavitary image acquisition under multimodal ultrasonography

To provide a basis for risk prediction, this paper combines conventional ultrasound, ultrasonography and shear wave elastography examination methods to acquire images of focal lesions in the renal cavity using multimodal ultrasonography.

3.1.1 Routine ultrasonographic methods for focal renal lesions

All two-dimensional ultrasound and ultrasonography examinations of focal renal lesions are performed by the same ultrasonographer with more than 10 years of experience in renal ultrasound diagnosis. Patients are placed in supine position with their hands held up over their heads to widen the rib cage. The examination is conducted by using Philips EPIQ8 ultrasound C4-1 convex array probe. Patients are fasted for about 5 hours and rested for 15 min before the examination. The routine ultrasound examination of the kidneys is carried out in the right subcostal, subxiphoid, left subcostal, right intercostal positions, and in the order of transverse sweep first and then longitudinal sweep. A comprehensive routine two-dimensional ultrasound examination of the renal tissue is first performed, followed by a focused examination of the detected focal renal lesions (Minnella et al.,2020). Furthermore, the location, size, shape, border, margin, interior, and posterior echogenicity of the lesion, presence of calcification and changes in surrounding tissue structures, blood flow and spectrum are marked.

3.1.2 Ultrasonography of focal lesions of the kidney

After patients completed informed consent signing, ultrasonography of focal renal lesions is performed using a Supersonic Imagine Aixplorer ultrasound SC5-2 convex array probe (Pitcairn et al.,2021). The specific operations are as follows.

(1) Ultrasound contrast agent administration. 3 mL of saline is drawn and set aside, and then the bottle is shaken to redistribute the microbubbles evenly. Draw 3mL Supersonic into a syringe and inject the mass into a peripheral vein. The spare 6mL saline mass is injected into the peripheral venous flush line.

(2) After 2D ultrasound has fully assessed the 2D ultrasound characteristics and color flow spectrum of the focal renal lesion, the largest and most clearly displayed section of the lesion is placed as far as possible in the center of the display, while the probe is immobilized. Moreover, the real-time ultrasonography mode is selected and the image to real-time dual-frame ultrasonography mode is adjusted. The image depth and gain is adjusted at the same time so that the best two-dimensional image is displayed.

(3) Injecting the pre-prepared ultrasound contrast agent into the peripheral vein, simultaneously, starting the timer on the screen. And launch dynamic video recording, followed by real-time dynamic observation of the ultrasonographic pattern of focal renal lesions.

(4) Dynamic observation and video recording lasted for 5 min.

3.1.3 Shear-wave elastography of focal renal lesions

After the patient rested 15 min from completing ultrasonography, shear-wave elastography is performed with the Supersonic Imagine Aixplorer ultrasound SC5-2 convex array probe (Ylca et al.,2021). The previous lesion is optimally displayed first, after which the elastography mode is selected for elastography examination. Large vessels and bile ducts are avoided as much as possible. The sample frame size is taken to include as much of the lesion and some of the surrounding renal tissue as possible. If the lesion is large, place the sampling frame in the center and at the edge of the lesion (including part of the lesion and part of the surrounding renal tissue). The patient is asked to hold his breath at the end of calm breathing and wait until the color image is as full as possible (larger than one-half of the sampling frame, niform, no mosaic). The images are accessed when the frame is fixed and stable for 4s. Young's modulus values of the lesion and surrounding renal tissue are measured and recorded. Young's modulus values for different tissues are measured using the machine's built-in quantitative analysis tools Q-Box and Q-Box Ratio. The hardness of the tissues in the images is indicated from hard to soft in red to blue, with higher Young's modulus values indicating harder tissues. The measurements are performed by using an area of interest of size 15 mm × 20 mm and the depth should be no greater than 65 mm.

3.2 Risk prediction model for the occurrence of AKI in sepsis

Based on the intracavitary images of the kidney acquired by multimodal ultrasonography, a knowledge-aware risk prediction model is designed. As shown in Figure 1. The model aims to use the existing medical knowledge theory to enrich the semantics of patient characteristics and to solve the problem of poor model prediction results caused by differences in the distribution of multicenter clinical data. Suppose the source dataset and the target dataset are D_s and D_t, The two data are from different clinical centers with different marginal data distributions, that is $P_{D_s}(x) \neq P_{D_t}(x)$. It may lead to significant reduction in predictive performance of the model in target dataset.

The supervised way of this risk prediction model is unsupervised. The model was first trained with patient data $D_s^l = \{(x_i, y_i)\}_{i=1}^{N_s}$ with the label of AKI occurring in sepsis and patient data $D_t^u = \{(x_i)\}_{i=1}^{N_t}$ without the label as a way to learn information about patient characteristics common to both the source and target datasets.

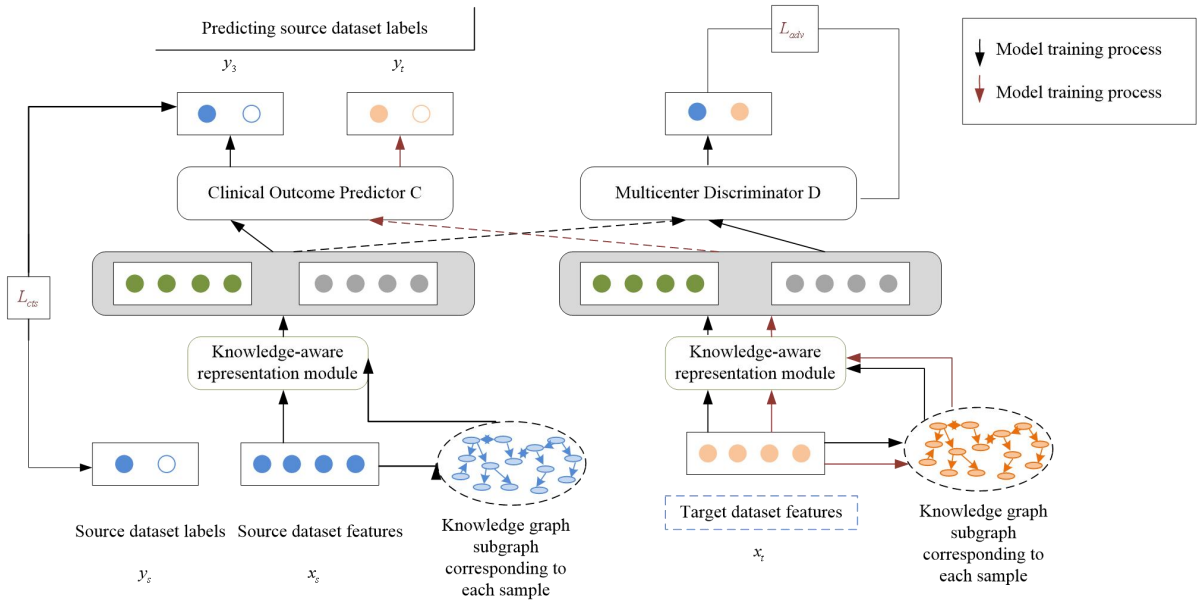

Figure 1 Schematic diagram of the risk prediction model

The proposed risk prediction model injects external knowledge graphs into feature mining of a multicenter clinical dataset. It is also validated by predicting the occurrence of AKI events in UFCH patients and MIMIC-III patients with sepsis. In this paper, learning and extracting features from each clinical center dataset are treated as independent tasks, and common features of multi-center patients are extracted by adversarial learning. At the same time, existing clinical knowledge from external knowledge graphs is introduced to enrich the semantics of patient features and complete the extraction of knowledge features. Besides, the personality features of patients are extracted by feature encoder. Finally, the relationship between personality and knowledge features is fully utilized through an attention mechanism based on knowledge perception for the prediction of such occurring in sepsis. Specifically, the constructed risk prediction model extracts patient features from specific clinical centers using a neural network to learn the relationship between the knowledge graph and the original patient features, and embeds them into a network model consisting of the following two parts:

(1) a multicenter discriminator that distinguishes patient features of the source and target datasets and extracts common features of multicenter clinical datasets through adversarial learning.

(2) a multilayer perceptron acts as a classifier for clinical outcome prediction. The risk prediction model is divided into three main modules, the knowledge feature extraction module, patient feature representation module, and the multicenter discriminator module based on adversarial learning. The following will describe the model construction process in detail from these three modules.

3.2.1 Knowledge feature extraction

To construct a knowledge map according to the obtained sepsis ultrasonography information. Assuming that the constructed knowledge graph is $g=(\varepsilon,R)$, where ε refers to the entities in the knowledge graph and R refers to the relationships between the entities in the knowledge graph.

Randomly restore the feature vector corresponding to the concept $e_i \in \varepsilon$ in each knowledge graph to the initial state. After that, generate new feature vectors through l layer GCN [26]. The GCN process is calculated by the following equation:

$$h_{e_i}=f\left(\sum_{r\in R}\sum_{j\in N_i^r}\frac{1}{\left|N_i^r\right|}W_r^{(1)}g_{e_i}+W_o^{(1)}g_{e_i}\right) \quad (1)$$

$$h_{e_i}=f\left(\sum_{r\in R}\sum_{j\in N_i^r}\frac{1}{\left|N_i^r\right|}W_r^{(1)}h_{e_i}^{(i-1)}+W_o^{(1)}h_{e_i}^{(i-1)}\right) \quad (2)$$

Where N_i^r denotes the set of neighboring nodes of entity concept e_i in relation r. $f(x)$ denotes the ReLU activation function, as shown in the following equation. $W_r^{(l)}$ denotes the weight matrix under the relationship at layer l, $W_o^{(l)}$ is the weight matrix of its own nodes at layer l, and $h_{e_i}^{(l)}\in R^{d_e}$ denotes the feature vector of concept e_i at layer l.

$$f(x)=\begin{cases}0 & if\ x<0\\ x & if\ x\geq 0\end{cases}$$

（3）

After organizing a large number of clinical concepts and transforming them into individual entities, the triad (e_i,r,e_j) is scored by DistMult factorization. e_i is the head node, e_j is the tail node, and r represents the relationship between two nodes. The scoring formula is shown below:

$$s(e_i,r,e_j)=\sigma\left(h_{e_i}^T R_r h_{e_j}\right)$$

（4）

Where $\sigma(x)$ is the sigmoid activation function h_{e_i}. $h_{e_j}\in R^{d_e}$ refers to the eigenvectors corresponding to the clinical concepts e_i and e_j.

For each correct triad $(v)\in K$ and incorrect triad $\left(e_i^r,r,e_j^r\right)\notin K$, the training model has a score size relationship of $s(e_i,r,e_j)>s\left(e_i^{'},r,e_j^{'}\right)$. The task of the training model is to distinguish between correct and incorrect triads, so the following cross-entropy function is chosen as the loss function for the described knowledge feature extraction module:

$$L_g=-\frac{1}{2|\Gamma|}\sum_{\langle(e_i,r,e_j),y\rangle\in\Gamma}\left(y\log s(e_i,r,e_j)+(1-y)\log\left(1-s(e_i,r,e_j)\right)\right)$$

（5）

Where L_g is the loss function of said knowledge feature extraction module, and $\langle(e_i,r,e_j),y\rangle$ represents the triad with the corresponding labels. When the triad (e_i,r,e_j) is included in the constructed knowledge graph, y takes the value of 1 and conversely y takes the value of 0. Γ represents the set of $\langle(e_i,r,e_j),y\rangle$. After completing the training of the knowledge graph and embedding it into the prediction model of acute kidney injury occurring in sepsis, the feature information in the patient samples $X_{s/t}$ included in the model is obtained by means of knowledge feature extraction.

3.2.2 Knowledge-aware based patient feature representation

After completing the extraction of knowledge features x^k, the potential knowledge feature representation z^k of the patient is extracted by encoding the knowledge features x^k through the encoder and combined with the decoder for reconstruction. The calculation formula is shown as follows:

$$\begin{cases}z^k=W_{k1}x^k+b_{k1}\\ \hat{x}^k=W_{k2}z^k+b_{k2}\end{cases}$$

（6）

Where W_{k1} indicates the weight matrix of the encoder, b_{k1} represents the bias of the encoder, W_{k2} denotes the weight matrix of the decoder. b_{k2} shows the bias of the decoder, z^k means the potential knowledge feature representation, and $\hat{x}^k$ refers to the reconstructed feature vector.

In this module, patient samples x^p and knowledge features x^k are respectively, to obtain patient feature representations z^p and knowledge feature representations z^k. Assuming a predictive model decoder of D_{rec}, the loss functions of the input x^k and reconstructed feature vectors $\hat{x}^k$ are calculated as shown below:

$$L_{rec}\left(x^k\right)=-\mathrm{E}_{x_k}\left(\left\|D_{rec}\left(z^k\right)-x^k\right\|_2^2\right)$$

（7）

To discover the relationship between patient feature representation z^p and knowledge feature representation z^k, an attention mechanism based on knowledge perception was designed. Assuming that the patient feature vector plays a different role in patient performance, the important features of patients are identified by the attention mechanism. The attention mechanism is computed as shown below:

$$M=\left(z^p\right)^T\cdot z^k$$

（8）

Where M is the correlation matrix of the patient sample, representing the dot product of z^p and z^k. $M_{i,j}$ represents the relationship between the i-th element of the patient feature representation z^p and the

j -th element of the knowledge feature representation z^k.

The normalized feature row vector a^p and the normalized feature column vector a^k are calculated using the SoftMax function for M. The formula is as follows:

$$\begin{cases} \alpha^p = SoftMax\left(\dfrac{\sum_{i=1}^{N} M[\cdot,i]}{N}\right) \\ \alpha^K = SoftMax\left(\dfrac{\sum_{i=1}^{N} M[j,\cdot]}{N}\right) \end{cases} \quad (9)$$

The extracted knowledge-aware patient-based feature representation matrix is B^p, and the patient-oriented knowledge feature representation matrix is B^k. Both are calculated as shown below Where U_{p1} and U_{k1} are projection parameters, $I^p, I^k = [1,\cdots 1]^T$ denote a N -dimensional all-1 vector, respectively. $\otimes$ refers to the Kronecker product operation, denotes the multiplication operation between elements.

$$\begin{cases} B^P = \tanh\left(U_{P1}\left(z^p + \left(I^P \otimes \alpha^P\right) \quad z^k\right)\right) \\ B^k = \tanh\left(U_{k1}\left(z^k + \left(I^k \otimes \alpha^k\right) \quad z^p\right)\right) \end{cases} \quad (10)$$

After obtaining B^P and B^k, this module generates a patient feature representation π^p containing knowledge and a patient-oriented knowledge feature representation π^k. This is calculated as follows:

$$\begin{cases} \pi^p = B^P \cdot z^p \\ \pi^k = B^K \cdot z^k \end{cases} \quad (11)$$

Ultimately, a knowledge-aware patient feature representation $\pi(x)$ corresponding to each patient sample x is obtained. Defined by the following expression:

$$\pi(x) = \left[\pi^p; \pi^k\right] \quad (12)$$

3.2.3 Multicenter discriminator based on adversarial learning

This module is an adversarial learning module for extracting common features of patient samples from the source and target datasets. Specifically, the module is assumed to have a multicenter discriminator D_{adv} that can be used to distinguish patient samples from the source dataset $\pi(x_s)$ and patient samples from the target dataset $\pi(x_t)$. A cross-entropy function is selected as the loss function for said discriminator D_{adv}. The formula is as follows.

$$L_{adv} = -\mathrm{E}_{x_s}\left(\log D_{adv}\left(\pi\left(x_s\right)\right)\right) - \mathrm{E}_{x_t}\left(\log\left(1 - D_{adv}\left(\pi\left(x_t\right)\right)\right)\right) \quad (13)$$

Assuming that the predictor of clinical outcome of the source dataset is c, the cross-entropy function is chosen as the loss function. The calculation formula is shown below:

$$L_{cls} = \mathrm{E}_{(x_s, y_s)}\left(-\sum_{k=1}^{k} \Pi\left(k = y_s\right) \log C\left(\pi\left(x_s\right)\right)\right) \quad (14)$$

Where K is the number of clinical outcome labels. Ultimately, the risk prediction model optimization is calculated as follows:

$$\Theta^* = \arg \min_{\Theta_\pi, \Theta_R, \Theta_c} \max_{\Theta_D} \left(L_{cls} + \lambda_1 L_{adv} + \lambda_2 L_{rec}\right) \quad (15)$$

Where λ_1 and λ_2 are hyperparameters.

4 RESULTS AND ANALYSIS

A prediction model for the risk of acute kidney injury in sepsis based on multimodal ultrasonography is applied to 100 patients with sepsis in a municipal hospital. Multiple indicators of clinical decision curve, sensitivity, specificity, accuracy, and AUC are selected to objectively

evaluate the validity and accuracy of the prediction model from multiple perspectives.

4.1 Risk prediction clinical decision curve

A risk prediction model is employed to obtain the probability of occurrence of acute kidney injury in one of the patients with sepsis. It is defined as positive when the probability of occurrence reaches a threshold and interventions are required. There will be benefits for the patient to be treated at this point (i.e., pros), as well as harms for the non-acute kidney injury patient to be treated with intervention and losses for the acute kidney injury patient to be left untreated (i.e., cons). The clinical decision curve shown in Figure 2 is drawn according to the risk prediction model. The vertical coordinate in Figure 2 is the net benefit after subtracting the disadvantages from the benefits. The bottom horizontal axis represents the threshold probability. The "ALL" line and the "None" line represent the two extreme cases. The "ALL" line indicates that if all samples are positive, i.e., all patients with sepsis develop acute kidney injury, then all patients receive the intervention and the net benefit is a backslope with a negative slope. The "None" line means that if all samples are predicted to be negative (i.e., the probability of occurrence is less than the threshold probability), i.e., none of the patients have acute kidney injury, then all patients with sepsis do not receive the intervention and the net benefit is zero. The risk prediction curve presents the model's prediction of the risk of acute kidney injury. The farther the curve is from the extremes of the "ALL" and "None" lines, the higher the clinical utility of the model. As shown by the trend of the three curves of the clinical decision graph, the application of the prediction model resulted in a net benefit for patients in the range of 0.017 to 0.89 for the threshold probability fluctuation compared to all patients with and without the intervention treatment. This indicates that the multimodal ultrasonography technique designed in this paper improves the validity of the acquired images of focal lesions in the renal cavity by combining conventional ultrasonography methods, ultrasonography methods, and shear wave elastography, thus conferring favorable clinical utility to the model.

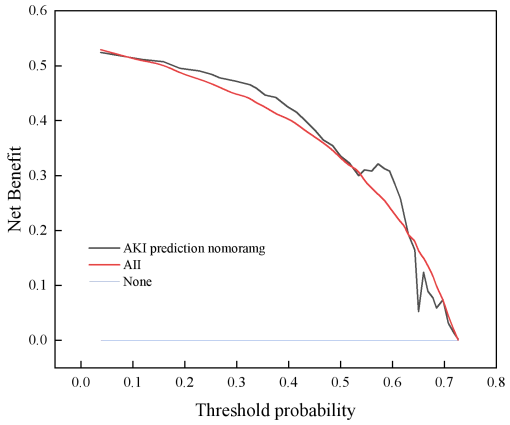

Figure 2 Clinical decision curve for the risk of acute kidney injury in patients with sepsis

4.2 Risk prediction model performance test

Five different prediction methods mentioned in the literature are selected in this session, namely, acute kidney injury prediction means based on plasma cystatin C and renal resistance index, biochemical indicators, creatinine levels, hematological ratios, and multivariate logistic regression analysis. The superiority of our method in predicting the risk of acute kidney injury in patients with sepsis was tested by comparing the prediction results of the five methods with the prediction results of our model. The results of the risk prediction performance test of each method are shown in Figure 3.

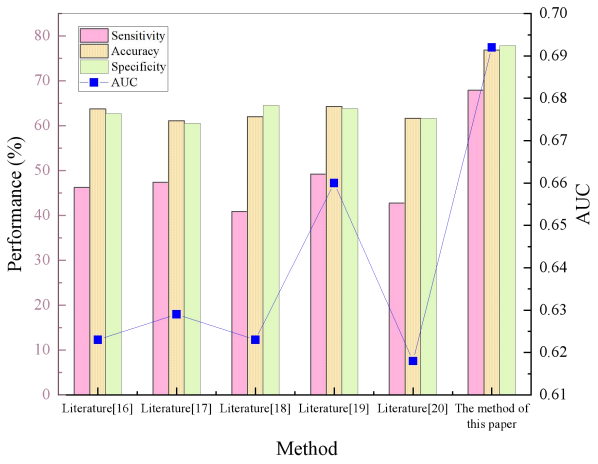

Figure 3 Schematic diagram of performance validation comparison of different prediction methods

From the results in Figure 3, it can be seen that the sensitivity, specificity, accuracy, and AUC of the method in this paper had high values of 67.9%, 82.48%, 76.86%, and 0.692, respectively. the method in Ref. (Raman et al.,2020) has the lowest sensitivity of 40.85%. The sensitivity of the other methods was 46.21%, 47.4%, 49.22%, and 42.78%, correspondingly. The above data indicate that the method in this paper has a better ability to predict the risk of acute kidney injury in patients with sepsis, while the comparison method has a weaker ability to do so. Regarding the two indicators of specificity and accuracy, the method of Ref. (Zdziechowska et al.,2021) has the smallest values, only 64.13% and 61.09%. The other four comparison methods had specificity values of 66.42%, 68.38%, 67.55%, and 65.29%, and accuracy of 63.78%, 62.05%, 64.27%, and 61.63%, respectively. This shows that the ability of the method in this paper to predict the risk of not developing acute kidney injury in patients with sepsis is also relatively strong, while the predictive ability of the comparison method is weaker. For the accuracy, the method in this paper also demonstrated the same extraordinary superiority relative to the comparison method, which was 15.77% higher than the lowest value. The AUC evaluation index, which is currently recognized as a better evaluation index, can accurately and clearly test the prediction performance of the method. The closer the value is to 1, the higher the authenticity of the method is. If it is equal to be 0.5, the authenticity is the lowest, and it does not have any application value at this time. After comparing the AUC values of the methods, it is found that the AUC values of both the comparison method and the method in this paper are greater than 0.5, indicating that each method has some feasibility. The AUC value of the method in Ref.(Trongtrakul et al.,2020) is the smallest, reaching only 0.618, which is much lower than the 0.692 of the method in this paper, indicating the significant predictive superiority of the model in this paper. In summary, this paper trains the model, learns patient feature information common to the source and target datasets based on intra-cavity images of the kidney acquired by multimodal ultrasonography, through data of patients with sepsis-onset acute kidney injury label and data of patients without sepsis-onset acute kidney injury label. The knowledge-aware attention-based mechanism makes full use of the relationship between patient personality traits and knowledge traits. Therefore, it makes the proposed model have a more desirable performance in predicting the risk of acute kidney injury occurring in sepsis, which can provide some guidance for the prevention and treatment of acute kidney injury occurring in sepsis patients. (Zeng et al.,2021)

5 DISCUSSION

The following limitations also exist in this study. Accurate prediction of high-risk patients and timely intervention and preventive measures are also current research hotspots in the field of critical care medicine. The next step of research can further select some biomarkers combined with prediction models for risk prediction of acute kidney injury to enhance the accuracy of prediction further. The sample of this study included only 1 hospital patient, and the sample size is small and unrepresentative as well as external validation is not performed. Subsequent multicenter studies can be conducted on the basis of expanding the sample size and adding external validation to augment the accuracy of the prediction model.

6 CONCLUSIONS

In this paper, a multimodal ultrasound imaging technique is constructed based on the diagnostic criteria for the occurrence of acute kidney injury in sepsis, combining conventional ultrasound examination methods, ultrasonography examination methods, and shear wave elastography examination methods. After converting the intra-cavity images of the kidney acquired by this technique into a knowledge map, the risk prediction of acute kidney injury occurring in sepsis patients is completed through the stages of knowledge feature extraction, patient feature representation, and multicenter discrimination by adversarial learning. After summarizing, the following conclusion points are drawn.

(1) The probability of acute kidney injury occurring in one of the sepsis patients is obtained using the risk prediction model, and a clinical decision curve is drawn.

The overall curve trend shows that the application of the prediction model resulted in net benefit for the patient with threshold probability fluctuations in the range of 0.017 to 0.89 when compared to all patients with and without interventional treatment.

(2) The predictive performance of patients with sepsis at risk of acute kidney injury is characterized by sensitivity. After comparing the sensitivity values of different methods, it is found that the sensitivity value of the model in this paper is as high as 67.9%, which indicates strong predictive ability in predicting the risk of developing acute kidney injury in sepsis patients.

(3) Specificity is employed to reflect the ability of predicting the risk of sepsis patients without acute kidney injury. The specificity index value of 82.48% for the model in this paper is much higher than that of the comparison method. Therefore, the ability of the model to predict the risk of sepsis patients without acute kidney injury is also relatively strong.

(4) For the comparison results of accuracy and AUC evaluation indexes, it is clear that the proposed model also demonstrates the same uncommon superiority and significant feasibility. The model makes full use of the relationship between patients' personality traits and knowledge traits according to the attention mechanism of knowledge perception. It resulted in an accuracy 15.77% higher than the lowest value and an AUC index value of 0.692.

DATA AVAILABILITY STATEMENT

The original contributions presented in the study are included in the article/supplementary material, further inquiries can be directed to the corresponding author.

REFERENCE

[1] Kunitsu, Y., Hira, D., Morikochi, A., Ueda, T., Isono, T., Morita, S. Y., & Terada, T. (2022). Time until onset of acute kidney injury by combination therapy with "Triple Whammy" drugs obtained from Japanese Adverse Drug Event Report database. *PloS one*, *17*(2), e0263682. https://doi.org/10.1371/journal.pone.0263682.

[2] Gong, Z. G., Zhao, Y., Wang, Z. Y., Fan, R. F., Liu, Z. P., & Wang, L. (2022). Epigenetic regulator BRD4 is involved in cadmium-induced acute kidney injury via contributing to lysosomal dysfunction, autophagy blockade and oxidative stress. *Journal of hazardous materials*, *423*(Pt A), 127110. https://doi.org/10.1016/j.jhazmat.2021.127110.

[3] Alejandra M T, Eduardo Z, Juan C, et al.(2022) MO336: Renal Recovery After Acute Kidney Injury Associated to COVID Requiring CRRT During ICU Hospitalization[J]. Nephrology Dialysis Transplantation, 2022(Supplement_3): Supplement_3.

[4] Shao, C. H., Tai, C. H., Lin, F. J., Wu, C. C., Wang, J. T., & Wang, C. C. (2022). Comparison of risk of acute kidney injury between patients receiving the combination of teicoplanin and piperacillin/tazobactam versus vancomycin and piperacillin/tazobactam. *Journal of the Formosan Medical Association = Taiwan yi zhi*, *121*(1 Pt 1), 117–125. https://doi.org/10.1016/j.jfma.2021.02.004.

[5] Xue, Q., Yang, L., Wang, H., & Han, S. (2021). Silence of Long Noncoding RNA SNHG14 Alleviates Ischemia/Reperfusion-Induced Acute Kidney Injury by Regulating miR-124-3p/MMP2 Axis. *BioMed research international*, *2021*, 8884438. https://doi.org/10.1155/2021/8884438.

[6] Hu, J., Gu, W., Ma, N., Fan, X., & Ci, X. (2022). Leonurine alleviates ferroptosis in cisplatin-induced acute kidney injury by activating the Nrf2 signalling pathway. *British journal of pharmacology*, *179*(15), 3991–4009. https://doi.org/10.1111/bph.15834.

[7] Zhang, Z. Y., Hou, Y. P., Zou, X. Y., Xing, X. Y., Ju, G. Q., Zhong, L., & Sun, J. (2020). Oct-4 Enhanced the Therapeutic Effects of Mesenchymal Stem Cell-Derived Extracellular Vesicles in Acute Kidney Injury. *Kidney & blood pressure research*, *45*(1), 95–108. https://doi.org/10.1159/000504368.

[8] Ig A, Ac B, La A, et al.(2021) Blood urea in preterm infants on routine parenteral nutrition: A multiple linear regression analysis[J]. Clinical Nutrition, 2021, 40(1):153-156.

[9] Lazzareschi, D., Mehta, R. L., Dember, L. M., Bernholz, J., Turan, A., Sharma, A., Kheterpal, S., Parikh, C. R., Ali, O., Schulman, I. H., Ryan, A., Feng, J., Simon, N., Pirracchio, R., Rossignol, P., & Legrand, M. (2023). Overcoming barriers in the design and implementation of clinical trials for acute kidney injury: a report from the 2020 Kidney Disease Clinical Trialists meeting. *Nephrology, dialysis, transplantation : official publication of the European Dialysis and Transplant Association - European Renal Association*, *38*(4), 834–844. https://doi.org/10.1093/ndt/gfac003.

[10] Zeng M, Cao Y, Xu R, et al.(2020) Oleanolic acid derivative isolated from Gardenia jasminoides var. radicans alleviates LPS-induced acute kidney injury in mice by reducing oxidative stress and inflammatory responses via the TLR4/NF-κB/NLRP3 signaling pathway[J]. New Journal of Chemistry, 2020, 44(5):2091-2101.

[11] Wu, P., Li, H., Zeng, N., & Li, F. (2022). FMD-Yolo: An efficient face mask detection method for COVID-19 prevention and control in public. *Image and vision computing*, *117*, 104341. https://doi.org/10.1016/j.imavis.2021.104341.

[12] N. Zeng, Z. Wang, H. Zhang, K.-E. Kim, Y. Li and X. Liu, (2019)"An improved particle filter with a novel hybrid proposal distribution for quantitative analysis of gold immunochromatographic strips, IEEE Transactions on Nanotechnology, vol. 18, no. 1, pp. 819-829, 2019.

[13] Zeng, N., Wang, Z., Zineddin, B., Li, Y., Du, M., Xiao, L., Liu, X., & Young, T. (2014). Image-based quantitative analysis of gold immunochromatographic strip via cellular neural network approach. *IEEE transactions on medical imaging*, *33*(5), 1129–1136. https://doi.org/10.1109/TMI.2014.2305394.

[14] Zeng, N., Wang, Z., Li, Y., Du, M., Cao, J., & Liu, X. (2013). Time Series Modeling of Nano-Gold

Immunochromatographic Assay via Expectation Maximization Algorithm. *IEEE transactions on bio-medical engineering*, *60*(12), 3418–3424. https://doi.org/10.1109/TBME.2013.2260160.

[15] González, J., Jatem, E., Roig, J., Valtierra, N., Ostos, E., Abó, A., Santacana, M., García, A., & Segarra, A. (2022). Usefulness of urinary biomarkers to estimate the interstitial fibrosis surface in diabetic nephropathy with normal kidney function. *Nephrology, dialysis, transplantation : official publication of the European Dialysis and Transplant Association - European Renal Association*, *37*(11), 2102–2110. https://doi.org/10.1093/ndt/gfac185.

[16] El-Sadek, A. E., El-Gamasy, M. A., Behiry, E. G., Torky, A. A., & Fathy, M. A. (2020). Plasma cystatin C versus renal resistive index as early predictors of acute kidney injury in critically ill neonates. *Journal of pediatric urology*, *16*(2), 206.e1–206.e8. https://doi.org/10.1016/j.jpurol.2019.12.001.

[17] Zdziechowska, M., Gluba-Brzózka, A., Franczyk, B., & Rysz, J. (2021). Biochemical Markers in the Prediction of Contrast-induced Acute Kidney Injury. *Current medicinal chemistry*, *28*(6), 1234–1250. https://doi.org/10.2174/0929867327666200502015749.

[18] Raman, S., Tai, C. W., Le Marsney, R., Schibler, A., Gibbons, K., & Schlapbach, L. J. (2020). Prediction of Acute Kidney Injury on Admission to Pediatric Intensive Care. *Pediatric critical care medicine : a journal of the Society of Critical Care Medicine and the World Federation of Pediatric Intensive and Critical Care Societies*, *21*(9), 811–819. https://doi.org/10.1097/PCC.0000000000002411.

[19] Titus D H, Meriem K, Saskia H, et al. MO313: Haematological Ratios as Risk Factor for Acute Kidney Injury in Patients Suspected of an Infection at the Emergency Department[J]. Nephrology Dialysis Transplantation, 2022(Supplement_3): Supplement_3.

[20] Trongtrakul, K., Patumanond, J., Kongsayreepong, S., Morakul, S., Pipanmekaporn, T., Akaraborworn, O., & Poopipatpab, S. (2020). Acute kidney injury risk prediction score for critically-ill surgical patients. *BMC anesthesiology*, *20*(1), 140. https://doi.org/10.1186/s12871-020-01046-2.

[21] Liu, Z., Xie, L., Qiu, K., Liao, X., Rees, T. W., Zhao, Z., Ji, L., & Chao, H. (2020). An Ultrasmall RuO2 Nanozyme Exhibiting Multienzyme-like Activity for the Prevention of Acute Kidney Injury. *ACS applied materials & interfaces*, *12*(28), 31205–31216. https://doi.org/10.1021/acsami.0c07886.

[22] Ostermann, M., Bellomo, R., Burdmann, E. A., Doi, K., Endre, Z. H., Goldstein, S. L., Kane-Gill, S. L., Liu, K. D., Prowle, J. R., Shaw, A. D., Srisawat, N., Cheung, M., Jadoul, M., Winkelmayer, W. C., Kellum, J. A., & Conference Participants (2020). Controversies in acute kidney injury: conclusions from a Kidney Disease: Improving Global Outcomes (KDIGO) Conference. *Kidney international*, *98*(2), 294–309. https://doi.org/10.1016/j.kint.2020.04.020.

[23] Minnella, G. P., Crupano, F. M., Syngelaki, A., Zidere, V., Akolekar, R., & Nicolaides, K. H. (2020). Diagnosis of major heart defects by routine first-trimester ultrasound examination: association with increased nuchal translucency, tricuspid regurgitation and abnormal flow in ductus venosus. *Ultrasound in obstetrics & gynecology : the official journal of the International Society of Ultrasound in Obstetrics and Gynecology*, *55*(5), 637–644. https://doi.org/10.1002/uog.21956.

[24] Pitcairn, C. F. M., & Kawka, M. (2021). Contrast-enhanced ultrasonography for intrahepatic cholangiocarcinoma: A cost-effective alternative for low-resource settings. *Hepatobiliary & pancreatic diseases international : HBPD INT*, *20*(3), 304–305. https://doi.org/10.1016/j.hbpd.2020.12.012.

[25] Ylca B, Ywk C, Hdw C, et al.(2021) The application of ultrasound shear wave elastography in the prediction of paradoxical upgrading reaction in tuberculous lymphadenitis. a pilot study - ScienceDirect[J]. Journal of the Formosan Medical Association, 2021.

[26] N. Zeng, P. Wu, Z. Wang, H. Li, W. Liu, X. Liu, (2022)A small-sized object detection oriented multi-scale feature fusion approach with application to defect detection, IEEE Transactions on Instrumentation and Measurement, vol. 71, article no. 3507014, 2022.